THE JOURNAL OF PHYSICAL CHEMISTRY C

Article

pubs.acs.org/JPCC

Cyclic Hydrogen Bonding in Indole Carboxylic Acid Clusters

Natalie A. Wasio,[†] Rebecca C. Quardokus,[†] Ryan D. Brown,[†] Ryan P. Forrest,[†] Craig S. Lent,[†,‡] Steven A. Corcelli,[†] John A. Christie,[†] Kenneth W. Henderson,[†] and S. Alex Kandel*[,†]

[†]Department of Chemistry and Biochemistry and [‡]Department of Electrical Engineering, University of Notre Dame, Notre Dame, Indiana 46556 United States

Supporting Information

ABSTRACT: Monolayers of indole-2-carboxylic acid and indole-3-carboxylic acid on gold are studied using ultrahigh-vacuum scanning tunneling microscopy. Both molecules form symmetric, cyclic, hydrogen-bonded pentamers, a structure that is stabilized by the presence of a weak hydrogen-bond donor (NH or CH) adjacent to the carboxylic acid on the five-membered ring. In addition to pentamers, indole-2-carboxylic acid forms hexamers and catemer chains, while indole-3-carboxylic acid monolayers are generally disordered. Density functional theory calculations show that pentamers and hexamers have stability comparable to dimers or short catemers. The coexistence of all of these structures likely arises from the nonequilibrium conditions present in solution during pulse deposition of the monolayer.

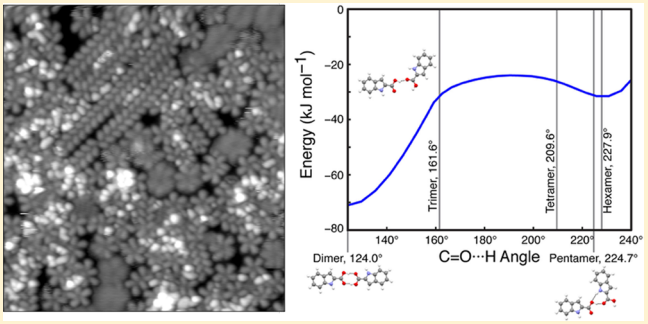

INTRODUCTION

Hydrogen bonds between carboxylic acids result in intermolecular forces that are strong, specific, and directional.[1] As a consequence of this, carboxylic acid hydrogen bonding plays a predominant role in determining the structure of proteins and of DNA. Following nature's lead, carboxylic acids are often used in systems engineered for self-assembly, resulting in a variety of supramolecular structures including dimers, catemer chains, and rings.[2−8] Of the three bonding motifs, rings are the rarest and dimers are significantly the most common. The catemer structure is usually less favored than the dimer, as it has lower entropy and is more susceptible to steric interference between bulky R substituents.[2,9] However, and also following nature's lead, the catemer structure can be promoted by the formation of a secondary hydrogen bond or by the introduction of other competitive hydrogen-bond donors and acceptors within the molecule.[10−12]

Hydrogen-bonded rings are essentially cyclic catemers. Poor packing in the solid state makes this bonding motif the least frequently observed. Until recently, catemer rings with 3, 4, or 6 molecules, trimers, tetramers, or hexamers, constituted the only known structures.[3] In addition to their presence in solid-state crystals, these rings have been observed on surfaces and studied by scanning tunneling microscopy (STM).[13,14]

In recent publications, we described the observation of a symmetric five-membered catemer ring of ferrocenecarboxylic acid, as well as the self-assembly of these pentamers to form a quasicrystalline monolayer.[15,16] The cyclic structure is stabilized by a weak CH···O hydrogen bond, created because the ring geometry places the 2-position C−H of one molecule (that is, the C−H adjacent to the COOH on the ring) in proximity to the carboxylic OH of its neighbor. In the current article, we show that this phenomenon is not unique to ferrocenecarboxylic acid and that symmetric, cyclic pentamers also form for indole-2-carboxylic acid (indole-2-COOH, Figure 1a); again, the pentamer is stabilized by the NH hydrogen-bond donor adjacent to the carboxylic acid on the five-membered ring. We describe our observations of one-dimensional catemer chains and five-membered rings stabilized by these secondary NH···O interactions. These structures are unlike those recently observed for this same molecule on graphite and Au(111) surfaces.[17] This is almost certainly due to significantly different methods of sample preparation and is a strong indication that the formation of certain structures within the monolayer depends on the kinetics of molecular adsorption and the nonequilibrium conditions present during a pulse deposition process.

EXPERIMENTAL SECTION

Au(111)-on-mica substrates were annealed, as well as sputtered in two cycles by Ar^+ ions at 400 °C. Indole-2-carboxylic acid and indole-3-carboxylic acid were purchased from Sigma-Aldrich and used as received or after purification using vacuum sublimation (Figure 6); the additional purification step did not produce observable differences in the samples formed. The indole compounds were dissolved in THF to make a ∼18 mM solution and were injected into a pulsed solenoid valve attached to the load lock of an ultrahigh-vacuum chamber. Microliters of solution were deposited into the chamber to adsorb onto the

Received: July 10, 2015
Revised: August 20, 2015
Published: August 24, 2015

DOI: 10.1021/acs.jpcc.5b06634
J. Phys. Chem. C 2015, 119, 21011−21017

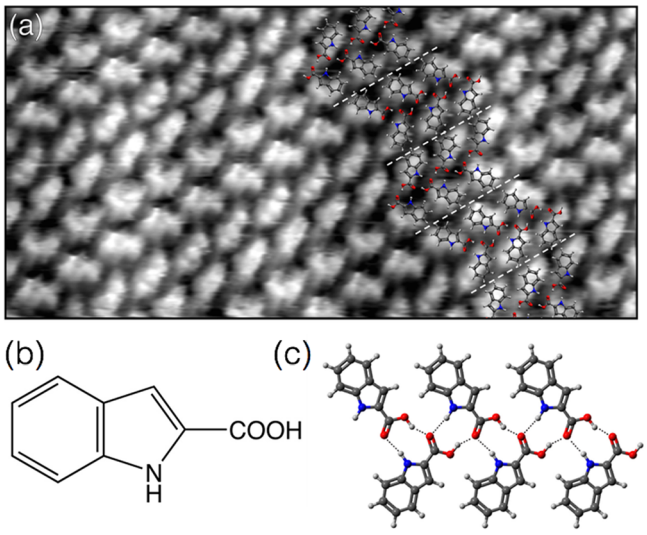

Figure 1. (a) Dense packing of indole-2-COOH with overlaid molecules to show the hydrogen bond packing arrangement, the slight disagreement between the overlaid molecules and underlying lattice in the image is due to drift within the scan; 120 Å × 60 Å, −1.5 V and 10 pA. White dashed lines separate each ribbon that changes directions. (b) Chemical structure of the indole-2-COOH. (c) Catemer structure with hydrogen bonding pattern.

annealed substrate at room temperature. After deposition, the substrate was immediately transferred into the main chamber and loaded into the sample stage of an Omicron LT-STM scanning tunneling microscope cooled to 77 K and operated at a base pressure of 10^{-10} Torr.

THEORETICAL CALCULATIONS

All calculations were performed using the Q-Chem software package. Density functional theory (DFT) is a computationally cost-effective alternative for describing hydrogen bonded systems when compared to more reliable but costly methods such as coupled-cluster theory with singles, doubles, and perturbative triples, CCSD(T). In accordance with our previous research on ferrocenecarboxylic acid hydrogen-bonded catemer systems, the Perdew, Burke, and Ernzerhof (PBE) density functional was chosen due to its relative accuracy for O−H···O hydrogen bonding. The 6-311++G(d, p) basis set was used for all atoms with a Lebedev quadrature containing 302 angular points with 100 radial shells in order to reduce numerical integration inaccuracies. To address basis set superposition error (BSSE), the Boys and Bernardi counterpoise correction method was used for each energy calculation. Geometries of the dimer and catemers were optimized while imposing respective C_{nh} symmetries, which aimed to keep the molecular systems planar as if they were bound to a surface. For the bent-dimer optimizations, the dimer OHO bond angle was increased in 5° increments, and the geometries were relaxed while imposing C_s symmetry, to enforce the same planarity while including the constrained angle.

RESULTS AND DISCUSSION

Scanning Tunneling Microscopy. Indole is a fused-ring heterocycle, consisting of a benzene ring joined to a pyrrole. Indole-2-COOH has a carboxylic acid group at the 2-position relative to the pyrrole nitrogen, and the most stable conformer has the carboxyl oriented on the same side of the amine. The crystal structure of indole-2-COOH shows that the molecule forms catemer chains in the solid state, with both NH and OH groups acting as hydrogen-bond donors.[18]

The general structure of the molecular rows observed on the surface is similar to the ribbon-like catemers seen in the solid state;[18] in particular, rows of molecules are always found in pairs. Paired rows are observed dispersed as well as alongside other pairs. In some cases, densely packed rows cover portions of the surface in a molecular monolayer, an example of which is shown in Figure 1a. Molecules appear to lie flat on the surface, and the "herringbone" reconstruction of Au(111) is undisturbed by molecular adsorption and is visible as three brighter vertical stripes in the image. Molecular overlays are shown along with the STM image to illustrate the packing arrangement of indole-2-COOH, with dashed white lines drawn between adjacent catemer ribbons, and the molecular packing direction reversing between adjacent ribbons. The same packing arrangement is expanded in Figure 1c to emphasize the hydrogen bonding between the molecules. This structure is quite similar to that observed in the crystal structure of indole-2-COOH.[18]

In addition to catemer rows, there are areas of the surface where STM images show significantly more complex structure, an example of which is shown in Figure 2. The surface contains a mixture of features including stripes, stars, and groups of mobile molecules that are blurred due to motion under the STM tip.

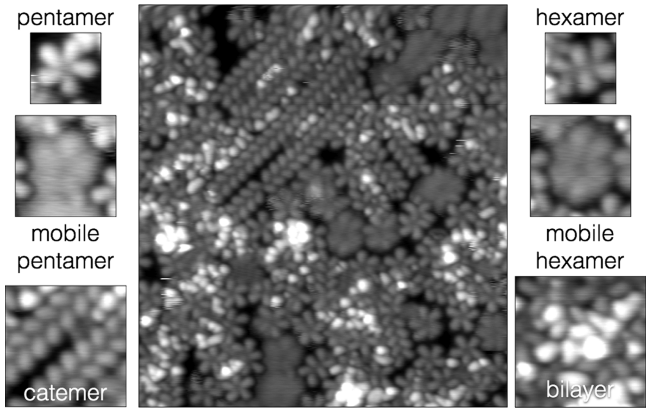

Figure 2. STM image (250 Å × 275 Å) of indole-2-COOH, acquired at −1 V and 10 pA. Pentamers and hexamers can be either sharply resolved or (because of motion on the surface) blurry. Catemer chains are also visible, as well as disordered regions corresponding to bilayers or aggregates of molecules and/or solvent.

While the zigzag hydrogen-bonding pattern of indole-2-COOH ribbons is present in the solid state, the stars in Figure 2 are a unique structure. The star-shaped features are produced when the carboxylic acid groups form a catemer ring of hydrogen bonds, as modeled in Figure 3b. The amine group provides a second hydrogen bond by acting as a hydrogen bond donor to the nearby hydroxyl oxygen. We have seen a similar bonding structure in ferrocenecarboxylic acid where an aromatic C−H bond acts as the hydrogen-bond donor.[15] Like ferrocenecarboxylic acid pentamers, close inspection of the star-shaped features (in Figure 2 as well as Supplemental Figure 1) shows them to be chiral. In the gas phase, clusters with the structure labeled as "R" and "S" in Supplemental Figure 1 are achiral and equivalent, but once adsorbed onto a surface the

DOI: 10.1021/acs.jpcc.5b06634
J. Phys. Chem. C 2015, 119, 21011−21017

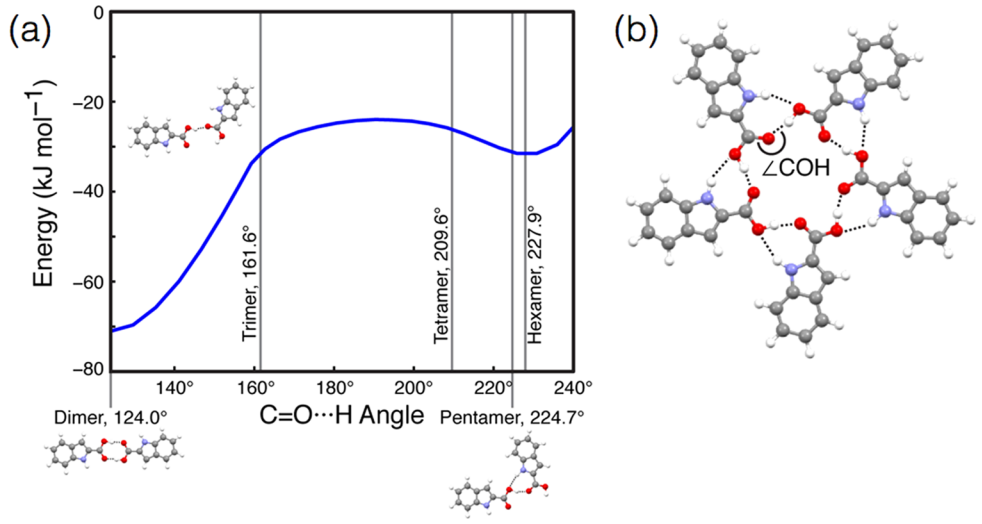

Figure 3. (a) Calculated energies for indole-2-COOH dimers as a function of CO···H bond angle. The deep minimum is for the dimer structure, while the shallow local minimum spans angles favorable for cyclic pentamer and hexamer formation. (b) Optimized geometry resulting from the DFT calculation of the full five-membered catemer ring.

horizontal mirror plane is lost, which renders the adsorbed species chiral. This is a common result of reduced dimensionality for molecular adsorbates.[19−21]

In addition to the catemer and cluster structures already discussed, images of indole-2-COOH also contain features that are blurry and diffuse. This type of feature blurriness is typical when imaged molecules are moving on the surface on a time scale that is fast relative to the STM scan rate. Such features seem to be found more frequently in less-densely packed regions of the monolayer, where intermolecular interactions are less likely to create barriers to rotational or translational molecular motion.[22] In our images, mobile clusters are blurry but retain discernible structures, and we attribute this blurriness to in-place pseudovibrational motion. An alternate explanation would be stochastic hopping between preferred orientations; these orientations, however, are unlikely to come from registry to the underlying substrate, as statistical analysis of images show an overall random distribution of pentamer orientations.

Density Functional Theory. DFT calculations were performed on a strained dimer system in order to determine the effect of secondary donors on hydrogen-bonded ring structures. The starting point for the calculation is an optimized, planar dimer geometry, which has two hydrogen bonds characterized by 124.0° CO···H bond angles. The structure was then reoptimized and the energy determined subject to a constraint on one of the CO···H angles, and the dependence of energy on bending angle is shown in Figure 3a. Bending of the dimer to increase the CO···H angle requires breaking one hydrogen bond and causes the energy to steadily increase. At an angle favorable to produce a trimer (161.6°), the energy continues to increase slowly and then begins to decrease at an angle between 190−195°. Increasing the angle further allows the N−H group to be close enough to interact and produce a secondary NH···O hydrogen bond; this is evident by the presence of a second energy minimum. This minimum contains both angles necessary to produce pentamers (224.7°) and hexamers (227.9°).

The constrained dimer calculation gives qualitative information about the presence of the second minimum; however, clusters with more than two molecules will form additional hydrogen bonds that are left dangling in the calculations used for Figure 3a. Accordingly, calculations for full cyclic structures were also performed. Table 1 gives the resulting cohesive energy for the trimer, tetramer, pentamer, and hexamer. The dimer remains as the energetically preferred structure; however, at room temperature both the pentamer and hexamer are within kT in energy. Depending on which stage of sample preparation the surface structure becomes kinetically locked, then, the coexistence of dimers, pentamers, and hexamers would be expected. Figure 2 shows the presence of pentamers, hexamers, and catemer chains of varying length, but there are no features that can unambiguously be assigned to the dimer. It is possible that the dimers are able to form other structures prior to becoming kinetically locked and thus are absent from the images.

Table 1. Calculated Energies for Indole-2-COOH for Clusters Having Two to Six Molecules

	cohesive energy per molecule (kJ/mol)
$(\text{indole-2-COOH})_2$	−35.5
$(\text{indole-2-COOH})_3$	−30.8
$(\text{indole-2-COOH})_4$	−29.2
$(\text{indole-2-COOH})_5$	−32.7
$(\text{indole-2-COOH})_6$	−33.8

The energy of the catemer was approximated using DFT calculations for progressively larger clusters; these clusters are arranged according to the catemer structure and then optimized. This approach is not as rigorously correct as a plane-wave calculation, where periodic boundary conditions would allow an effectively infinitely long catemer to be modeled. However, the methodology is identical to that used for the dimer and cyclic cluster calculations described previously, allowing the results to be compared quantitatively. A simple model of the effects of finite catemer length assumes an energy penalty for the ends (due to decreased hydrogen bonding opportunities) that is independent of chain length. The cohesive energy per molecule should then have a $1/n$ dependence, which Figure 4 shows matches the calculation exceedingly well. Figure 4 also illustrates that the cluster structures (dimer and cylic pentamer and hexamer) are lower in

DOI: 10.1021/acs.jpcc.5b06634
J. Phys. Chem. C 2015, 119, 21011−21017

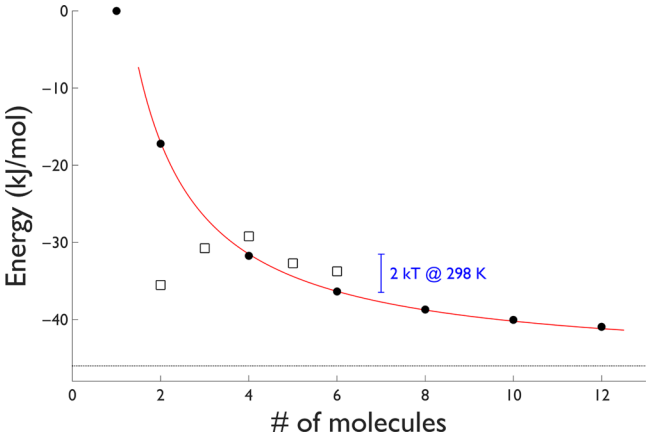

Figure 4. Calculated cohesive energy per molecule for catemer chains containing n = 2−12 molecules (filled black circles), with a $E_0 - E_p/n$ fit (solid line); the horizontal dotted line marks the E_0 asymptote of the catemer calculations. Open squares show the energy per molecule for dimers and ring-shaped clusters from Table 1. The scale bar (blue) is $2kT$ (4.96 kJ/mol) at room temperature.

energy than catemer chains of fewer than 6 molecules and that above 6 molecules catemers are predicted to be the lowest-energy structure.

Comparison of Indole-2-COOH and Indole-3-COOH. With the carboxylic acid group of indole-2-COOH located at the 2-position, the adjacent C−H and N−H groups compete to produce a secondary hydrogen bond in a cyclic structure. Typically, N−H groups are stronger hydrogen bonding donors compared to C−H groups, and it is assumed that they are responsible for stabilizing cyclic structures. To test for this, we imaged indole-3-carboxylic acid (indole-3-COOH). The carboxylic acid is now placed in the third position leaving a C−H group adjacent and the N−H further away. In a crystal, indole-3-COOH forms a sheet structure of dimers with some N−H interactions with nearby carboxyl oxygens.[23]

The conformation of indole-3-COOH in the solid-state crystal structure is drawn as conformation 1 in Figure 5a. When adsorbed on a surface, indole-3-COOH shows some disordered dimers along with scattered pentamers, Figure 5c. An individual pentamer is shown in the inset.

In comparison to indole-2-COOH, indole-3-COOH adsorption is characterized by less order and fewer pentamers. DFT calculations show that the energy depends on the overall conformation of the molecule. Flipping the carboxylic acid group of conformation 1 produces the geometry of conformation 2, Figure 5a. Energy versus C═O···H angle calculations for both conformations are plotted in Figure 5b. Both indole-3-COOH conformations (red and black curves) have deep minimum-energy structures for the dimer configuration. However, only conformation 2 (red curve) has a local minimum for cyclic pentamer and hexamer geometries. The location of this minimum is nearly identical to that calculated for indole-2-COOH (dashed blue curve), though the indole-2-COOH well is deeper, as would be expected given that NH is a better hydrogen-bond donor than CH. Conformation 1 (black curve) energies begin to diverge from conformation 2 when the geometry exceeds 180° and increase rapidly past that point.

The presence or absence of a second minimum for each conformation of indole-3-COOH depends on the location of the secondary hydrogen bond donor, Figure 5d. For conformation 1, the secondary hydrogen bond donor is an aromatic C−H from the benzene ring, whereas the C−H adjacent to the carboxylic acid group of the pyrrole ring is responsible for secondary interactions. Steric repulsion could

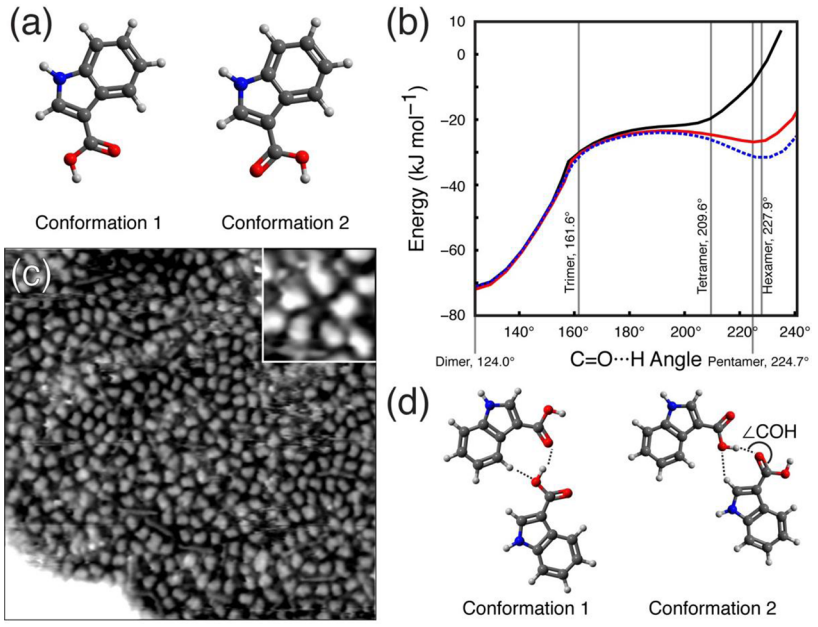

Figure 5. (a) Molecular models of indole-3-COOH in two conformations. A 180° rotation of the carboxylic acid group of conformation 1 produces the geometry of conformation 2. (b) Calculated energies for both conformers of indole-3-COOH dimers (black and red) as a function of CO···H bond angle. Indole-2-COOH energies are included and shown as a dashed, blue line. A second minima near pentamer and hexamer favored geometries is shown for conformation 2 (red) and absent for conformation 1 (black). (c) STM image (200 Å × 200 Å) of indole-3-COOH showing scattered groupings of five-membered rings. Image acquired at −1 V and 10 pA. An individual pentamer is shown in the inset, 28 Å × 28 Å. (d) Geometry of both indole-3-COOH conformations. Pentamer formation is favorable when secondary hydrogen bond interactions come from the pyrrole ring (conformation 2) rather than the benzene ring (conformation 1).

DOI: 10.1021/acs.jpcc.5b06634
J. Phys. Chem. C 2015, 119, 21011−21017

also play a role in the energy increase observed for conformation 1, as a further increase in C═O···H angle (toward hexamer favored angles) increases energy still. Even for conformation 2, however, the depth of the second minimum in Figure 5c is not as deep as the well depth for indole-2-COOH; this matches chemical intuition that N−H should be a better H-bond donor than C−H and potentially explains the greater incidence of pentamers for indole-2-COOH.

Adsorption and Assembly. For indole-2-COOH, the main image of Figure 2 shows multiple structures, including catemers, pentamers, hexamers, and less-ordered and disordered areas. This is a strong indication that the system is kinetically trapped and has not reached a state of minimum free energy. Kinetic constraints are not surprising given the method used for monolayer preparation, pulsed deposition from solution; in this process, a solenoid valve aimed at the surface injects small droplets of solution directly into vacuum. Rapid evaporation of solvent leads to supersaturation and significant cooling and has the potential to create gradients in concentration and temperature.[24−28]

This conclusion is reinforced by the fact that changing the deposition method used to create the monolayer results in a dramatically different structure. De Marchi et al. have studied the identical system, indole-2-carboxylic acid on Au(111), using vacuum sublimation to create the monolayer, and they report only close-packed monolayers, with no evidence of star-shaped pentamers or of hexamers.[17] They observe similar close-packed structure when monolayers are produced on a graphite surface using solution-phase deposition and imaging in inert liquid. The close-packed structure we see in Figure 1 is quite similar to that reported in ref 17, where it was described as close-packed rows of COOH dimers. We prefer the assignment of catemers for the structure produced in our experiments, as this is supported by the observation of isolated chains in Figure 2 and Supplemental Figure 2, which demonstrates that the repeating element in a single chain is chevron-shaped instead of a linear dimer.

Thermal annealing can be used to identify metastable structures, as higher temperatures provide the thermal energy to overcome barriers to rearrangement. Accordingly, we annealed samples immediately after pulse deposition for 30 min at temperatures of 42 and 65 °C, after which the samples were allowed to cool before being transferred to the microscope and imaged. Regions of roughly similar coverage are compared in Figure 6. Annealing results in a marked increase in the number of pentamers observed: they are the majority ordered species after the 42 °C anneal and the only remaining ordered features after annealing at 65 °C. Correspondingly, hexamers disappear almost completely after the 42 °C annealing step, while 65 °C eliminates catemers as well. Annealing also appears to increase the number of bright features we associate with disordered regions or bilayers. Apparent coverage of indole-2-COOH decreases with increasing annealing temperature, which indicates some molecular desorption occurs during the annealing stages.

The straightforward interpretation of these results is that hexamers are metastable with respect to pentamers. Hexamers are formed during pulse deposition and are kinetically trapped, and the barrier to conversion to pentamers can be overcome at 42 °C but not at room temperature. An interesting corollary to this is that hexamers cannot form through simple combination of an adsorbed molecule with an adsorbed pentamer, as the lower free energy of the pentamer requires a higher barrier for pentamer-to-hexamer than for hexamer-to-pentamer conversion. We have proposed that cluster formation in ferrocene carboxylic acids occurs in the solution phase (including the possibility of formation on the surface while still within the solvent droplet)[15,16] because of nonequilibrium conditions, low temperatures and high concentrations, produced during the pulse deposition process. The precipitation of indole-2-COOH pentamers and hexamers directly from solution remains a plausible explanation for the observation of these structures in our experiments. For ferrocene dicarboxylic acid, solution-phase clustering followed by precipitation appears to be the only acting mechanism for cluster formation.[29] Clearly this is not the case for indole-2-COOH, where rearrangement on the surface to create new pentamers is necessary to explain the increase in these features that accompanies annealing.

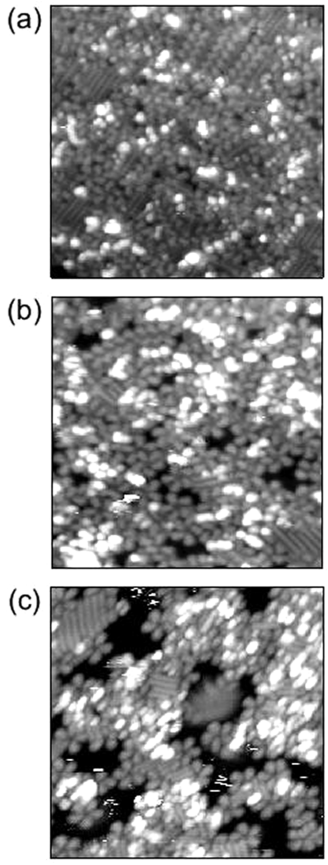

Figure 6. STM images of indole-2-COOH, all 195 Å × 195 Å in size and acquired at +1 V and 10 pA. Image (a) shows a sample as deposited via pulsed deposition with no further treatment. The sample imaged in (b) was annealed for 30 min at 42 °C. The frequency of pentamers has increased, while some catemers are still observed. In (c), the sample has been annealed for 65 °C for 30 min, after which most ordered molecular clusters now have the pentamer structure. All images were acquired at 77 K.

Annealing temperatures higher than 65 °C lead to a sharp decrease in surface coverage, and at no point do we observe the conversion of pentamers into catemer chains. While this might indicate that the catemers are metastable with respect to pentamers, this is not a plausible explanation, as catemers (1) match the solid-state structure, (2) are the only structure observed in ref 17, and (3) are predicted by our DFT calculations to be significantly lower in energy at longer chain lengths. Instead, we suggest that elevated temperatures activate

DOI: 10.1021/acs.jpcc.5b06634
J. Phys. Chem. C 2015, 119, 21011−21017

deprotonation of the indole-2-COOH carboxylic acid group. The substrate metal catalyzes the thermally initiated deprotonation of an adsorbed carboxylate species, yielding a carboxylate and a proton, the latter of which is eventually thermally desorbed as molecular hydrogen.[30,31] This process is known to drive irreversible phase or structural transformations for various carboxylic acids on metals,[32−36] and a mixture of protonated and deprotonated species at an interface can lead to the coexistence of different supramolecular structures.[35,37,38] Deprotonation of indole-2-COOH will likely disrupt the hydrogen bonding network necessary for catemer formation. A sufficient concentration of carboxylate species, then, would effectively impose a length limit for catemer growth, at which point the trend shown in Figure 5 (catemers are the lowest-energy structure only when $n \geq 6$) could drive pentamer formation. While it is possible that pentamers are able to incorporate carboxylates and catemers are not, we do not see any change in contrast or symmetry of pentamer features upon annealing. It is unlikely that deprotonation occurs without annealing (very unusual for gold surface, though anthraquinone-2-COOH is an exception[39]), as De Marchi et al. would likely also have observed pentamers in this case.

Finally, while both indole-2-COOH and indole-3-COOH assemble into cyclic pentamers similar in structure to those of ferrocenecarboxylic acid, neither indole monolayer displays the quasicrystallinity observed for that system. This supports the model of quasicrystal formation in which each pair of neighboring pentamers was bound together by their mutual edge−face interactions with a molecular dimer, allowed by a serendipitous matching of the dimer and pentamer geometries not likely to be found in other systems. Additional factors may play a role, including the formation of far fewer indole dimers (presumably due to the availability of the lower-energy catemer structure) and potential differences in the relative mobility of clusters once adsorbed onto the surface.

CONCLUSIONS

In conclusion, secondary hydrogen bonds drive the formation of cyclic pentamers for two indole carboxylic acid systems. Two hydrogen bond donors (N−H and C−H) adjacent to the carboxylic acid group of indole-2-COOH compete toward pentamer formation. In the indole-3-COOH system, only a C−H group adjacent to the carboxylic acid group can participate. Of the two molecular conformations tested for indole-3-COOH, only conformation 2 led to an additional energy minimum that favored pentamer and hexamer geometries similar to what was observed for indole-2-COOH. In both systems, the location of the secondary hydrogen bond donating group is the driving factor for the formation of pentamers. The pentamers likely form in solution and exist at the surface as a kinetically trapped metastable species, and annealing this surface results in the deprotonation of some of the carboxylic acid groups and the formation of additional pentamer clusters. The observation of pentamer clusters can be attributed to the presence of carboxylic acid groups with adjacent hydrogen bond donors, and this behavior should be generally applicable to self-assembly processes during solution-based deposition.

ASSOCIATED CONTENT

Supporting Information

The Supporting Information is available free of charge on the ACS Publications website at DOI: 10.1021/acs.jpcc.5b06634.

Additional STM images (S1) illustrate the handedness of adsorbed indole-2-COOH pentamers and (S2) show edges of catemer chains, supporting the assignment of structure as catemers rather than dimers (PDF)

AUTHOR INFORMATION

Corresponding Author

*E-mail: skandel@nd.edu.

Notes

The authors declare no competing financial interest.

ACKNOWLEDGMENTS

Support for this work has been provided by the National Science Foundation (NSF Grant No. CHE-1124762)

REFERENCES

(1) Steiner, T. The hydrogen bond in the solid state. *Angew. Chem., Int. Ed.* **2002**, *41*, 48−76.

(2) Beyer, T.; Price, S. Dimer or catemer? Low-energy crystal packings for small carboxylic acids. *J. Phys. Chem. B* **2000**, *104*, 2647−2655.

(3) Ivasenko, O.; Perepichka, D. Mastering fundamentals of supramolecular design with carboxylic acids. Common lessons from X-ray crystallography and scanning tunneling microscopy. *Chem. Soc. Rev.* **2011**, *40*, 191−206.

(4) Gatti, R.; MacLeod, J. M.; Lipton-Duffin, J. A.; Moiseev, A. G.; Perepichka, D. F.; Rosei, F. Substrate, Molecular Structure, and Solvent Effects in 2D Self-Assembly via Hydrogen and Halogen Bonding. *J. Phys. Chem. C* **2014**, *118*, 25505−25516.

(5) MacLeod, J. M.; Ben Chaouch, Z.; Perepichka, D. F.; Rosei, F. Two-Dimensional Self-Assembly of a Symmetry-Reduced Tricarboxylic Acid. *Langmuir* **2013**, *29*, 7318−7324.

(6) Lipton-Duffin, J.; Miwa, J. A.; Urquhart, S. G.; Contini, G.; Cossaro, A.; Casalis, L.; Barth, J. V.; Floreano, L.; Morgante, A.; Rosei, F. Binding Geometry of Hydrogen-Bonded Chain Motif in Self-Assembled Gratings and Layers on Ag(111). *Langmuir* **2012**, *28*, 14291−14300.

(7) Slater (Nee Phillips), A. G.; Beton, P. H.; Champness, N. R. Two-dimensional supramolecular chemistry on surfaces. *Chem. Sci.* **2011**, *2*, 1440−1448.

(8) Slater, A. G.; Perdigao, L. M. A.; Beton, P. H.; Champness, N. R. Surface-Based Supramolecular Chemistry Using Hydrogen Bonds. *Acc. Chem. Res.* **2014**, *47*, 3417−3427.

(9) Leiserowitz, L. Molecular packing modes - Carboxylic-acids. *Acta Crystallogr., Sect. B: Struct. Crystallogr. Cryst. Chem.* **1976**, *32*, 775−802.

(10) Kuduva, S.; Craig, D.; Nangia, A.; Desiraju, G. Cubanecarboxylic acids. Crystal engineering considerations and the role of CH···O hydrogen bonds in determining OH···O networks. *J. Am. Chem. Soc.* **1999**, *121*, 1936−1944.

(11) Das, D.; Jetti, R.; Boese, R.; Desiraju, G. Stereoelectronic effects of substituent groups in the solid state. Crystal chemistry of some cubanecarboxylic and phenylpropiolic acids. *Cryst. Growth Des.* **2003**, *3*, 675−681.

(12) Desiraju, G. C-H···O and other weak hydrogen bonds. From crystal engineering to virtual screening. *Chem. Commun.* **2005**, 2995−3001.

(13) MacLeod, J.; Ivasenko, O.; Fu, C.; Taerum, T.; Rosei, F.; Perepichka, D. Supramolecular ordering in oligothiophene-fullerene monolayers. *J. Am. Chem. Soc.* **2009**, *131*, 16844−16850.

(14) Xiao, W.; Jiang, Y.; Aiet-Mansour, K.; Ruffieux, P.; Gao, H.; Fasel, R. Chiral biphenyldicarboxylic acid networks stabilized by hydrogen bonding. *J. Phys. Chem. C* **2010**, *114*, 6646−6649.

(15) Wasio, N.; Quardokus, R.; Forrest, R.; Lent, C.; Corcelli, S.; Christie, J.; Henderson, K.; Kandel, S. Self-assembly of hydrogen-bonded two-dimensional quasicrystals. *Nature* **2014**, *507*, 86−89.

(16) Quardokus, R.; Wasio, N.; Christie, J.; Henderson, K.; Forrest, R.; Lent, C.; Corcelli, S.; Kandel, S. Hydrogen-bonded clusters of

DOI: 10.1021/acs.jpcc.5b06634
J. Phys. Chem. C 2015, 119, 21011−21017

ferrocenecarboxylic acid on Au(111). *Chem. Commun.* **2014**, *50*, 10229−10232.
(17) De Marchi, F.; Cui, D.; Lipton-Duffin, J.; Santato, C.; MacLeod, J.; Rosei, F. Self-assembly of indole-2-carboxylic acid at graphite and gold surfaces. *J. Chem. Phys.* **2015**, *142*, 101923.
(18) Morzyk-Ociepa, B.; Michalska, D.; Pietraszko, A. Structures and vibrational spectra of indole carboxylic acids. Part I. Indole-2-carboxylic acid. *J. Mol. Struct.* **2004**, *688*, 79−86.
(19) McGuire, A.; Jewell, A. D.; Lawton, T.; Murphy, C.; Lewis, E.; Sykes, E. Hydrogen bonding and chirality in functionalized thioether self-assembly. *J. Phys. Chem. C* **2012**, *116*, 14992−14997.
(20) Elemans, J. A. A. W.; De Cat, I.; Xu, H.; De Feyter, S. Two-dimensional chirality at liquid-solid interfaces. *Chem. Soc. Rev.* **2009**, *38*, 722−736.
(21) Raval, R. Chiral expression from molecular assemblies at metal surfaces: insights from surface science techniques. *Chem. Soc. Rev.* **2009**, *38*, 707−721.
(22) Gimzewski, J.; Joachim, C.; Schlittler, R.; Langlais, V.; Tang, H.; Johannsen, I. Rotation of a single molecule within a supramolecular bearing. *Science* **1998**, *281*, 531−533.
(23) Smith, G.; Wermuth, U.; Healy, P. Indole-3-carboxylic acid. *Acta Crystallogr., Sect. E: Struct. Rep. Online* **2003**, *E59*, o1766−o1767.
(24) Rabani, E.; Reichman, D.; Geissler, P.; Brus, L. Drying-mediated self-assembly of nanoparticles. *Nature* **2003**, *426*, 271−274.
(25) Deegan, R.; Bakajin, O.; Dupont, T.; Huber, G.; Nagel, S.; Witten, T. Capillary flow as the cause of ring stains from dried liquid drops. *Nature* **1997**, *389*, 827−829.
(26) Elbaum, M.; Lipson, S. How does a thin wetted film dry up. *Phys. Rev. Lett.* **1994**, *72*, 3562−3565.
(27) Smith, J. D.; Cappa, C. D.; Drisdell, W. S.; Cohen, R. C.; Saykally, R. J. Raman thermometry measurements of free evaporation from liquid water droplets. *J. Am. Chem. Soc.* **2006**, *128*, 12892−12898.
(28) Drisdell, W. S.; Saykally, R. J.; Cohen, R. C. On the evaporation of ammonium sulfate solution. *Proc. Natl. Acad. Sci. U. S. A.* **2009**, *106*, 18897−18901.
(29) Quardokus, R. C.; Wasio, N. A.; Brown, R. D.; Christie, J. A.; Henderson, K. W.; Forrest, R. P.; Lent, C. S.; Corcelli, S. A.; Kandel, S. A. Hydrogen-bonded clusters of 1,1′-ferrocenedicarboxylic acid on Au(111) are initially formed in solution. *J. Chem. Phys.* **2015**, *142*, 101927.
(30) Chen, Q.; Frankel, D.; Richardson, N. Dehydrogenation induced phase transitions of p-aminobenzoic acid on Cu(110). *J. Chem. Phys.* **2002**, *116*, 460−470.
(31) Immaraporn, B.; Ye, P.; Gellman, A. The transition state for carboxylic acid deprotonation on Cu(100). *J. Phys. Chem. B* **2004**, *108*, 3504−3511.
(32) Stepanow, S.; Strunskus, T.; Lingenfelder, M.; Dmitriev, A.; Spillmann, H.; Lin, N.; Barth, J.; Woll, C.; Kern, K. Deprotonation-driven phase transformations in terephthalic acid self-assembly on CU(100). *J. Phys. Chem. B* **2004**, *108*, 19392−19397.
(33) Ruben, M.; Payer, D.; Landa, A.; Comisso, A.; Gattinoni, C.; Lin, N.; Collin, J.-P.; Sauvage, J.-P.; De Vita, A.; Kern, K. 2D supramolecular assemblies of benzene-1,3,5-triyl-tribenzoic acid: Temperature-induced phase transformations and hierarchical organization with macrocyclic molecules. *J. Am. Chem. Soc.* **2006**, *128*, 15644−15651.
(34) Schwarz, D.; van Gastel, R.; Zandvliet, H. J. W.; Poelsema, B. In Situ Observation of a Deprotonation-Driven Phase Transformation: 4,4′-Biphenyldicarboxylic Acid on Au(111). *J. Phys. Chem. C* **2013**, *117*, 1020−1029.
(35) Classen, T.; Lingenfelder, M.; Wang, Y.; Chopra, R.; Virojanadara, C.; Starke, U.; Costantini, G.; Fratesi, G.; Fabris, S.; de Gironcoli, S.; et al. Hydrogen and coordination bonding supramolecular structures of trimesic acid on Cu(110). *J. Phys. Chem. A* **2007**, *111*, 12589−12603.
(36) Yeo, B.; Chen, Z.; Sim, W. Surface functionalization of Ni(111) with acrylate monolayers. *Langmuir* **2003**, *19*, 2787−2794.
(37) Mahapatra, M.; Burkholder, L.; Bai, Y.; Garvey, M.; Boscoboinik, J. A.; Hirschmugl, C.; Tysoe, W. T. Formation of Chiral Self-Assembled Structures of Amino Acids on Transition-Metal Surfaces: Alanine on Pd(111). *J. Phys. Chem. C* **2014**, *118*, 6856−6865.
(38) Kittelmann, M.; Rahe, P.; Gourdon, A.; Kuehnle, A. Direct Visualization of Molecule Deprotonation on an Insulating Surface. *ACS Nano* **2012**, *6*, 7406−7411.
(39) Han, S.; Joo, S.; Ha, T.; Kim, Y.; Kim, K. Adsorption characteristics of anthraquinone-2-carboxylic acid on gold. *J. Phys. Chem. B* **2000**, *104*, 11987−11995.

DOI: 10.1021/acs.jpcc.5b06634
J. Phys. Chem. C 2015, 119, 21011−21017